2

Quarterly Technical Report No. 1

Covering the Period 20 September 1971 - 31 January 1972

(NASA-CR-126674) DEVELOPMENT OF GaAs SOLAR CELLS Quarterly Technical Report, 20 Sep. 1971 - 31 Jan. 1972 P.J. McNally (Ion Physics Corp.) Mar. 1972 38 p CSCL 10A G3/03 N72-24047 Unclas 28186

DEVELOPMENT OF GaAs SOLAR CELLS

Contract No. 953270

Jet Propulsion Laboratory
California Institute of Technology
4800 Oak Grove Drive
Pasadena, California 91103

Approved by: Charles R. Lamar Jr.

F. T. C. Bartels
Division Manager

Philip J. McNally

Philip J. McNally
Principal Investigator

March 1972

ION PHYSICS CORPORATION IPC

A Subsidiary of High Voltage Engineering Corporation

BURLINGTON, MASSACHUSETTS

This report contains information prepared by Ion Physics Corporation under JPL Subcontract. Its content is not necessarily endorsed by the Jet Propulsion Laboratory, California Institute of Technology, or the National Aeronautics and Space Administration.

Quarterly Technical Report No. 1

Covering the Period 20 September 1971 - 31 January 1972

DEVELOPMENT OF GaAs SOLAR CELLS

Contract No. 953270

Jet Propulsion Laboratory
California Institute of Technology
4800 Oak Grove Drive
Pasadena, California 91103

Approved by:

F. T. C. Bartels
Division Manager

Philip J. McNally
Principal Investigator

This work was performed for the Jet Propulsion Laboratory, California Institute of Technology, sponsored by the National Aeronautics and Space Administration under Contract NAS7-100.

ION PHYSICS CORPORATION
BURLINGTON, MASSACHUSETTS

SUMMARY

During this report period refinement of calculations of GaAs solar cell output parameters and development of a computer model for parameter optimization was completed. The results were analyzed to determine the material characteristics required for a high efficiency solar cell. Calculated efficiencies for a P/N cell polarity are higher than an N/P cell. Both cell polarities show efficiency to have a larger dependence on short-circuit current than an open-circuit voltage under nearly all conditions considered. The tolerances and requirements of a cell fabrication process are more critical for an N/P type than for a P/N type cell. A cell efficiency of 20% should be possible in GaAs. Several solar cell fabrication considerations relative to junction formation using ion implantation are also discussed.

TABLE OF CONTENTS

Section		Page
1	INTRODUCTION	1
2	COMPUTER MODEL	4
	2.1 Computer Model Results	8
	2.1.1 P/N Cell Polarity	8
	2.1.2 N/P Cell Polarity	19
	2.1.3 Conclusions	19
3	SOLAR CELL FABRICATION CONSIDERATIONS	24
	3.1 P/N Junction Formation	24
4	FUTURE WORK	29
	REFERENCES	30

LIST OF ILLUSTRATIONS

Figure		Page
1	Absorption Coefficient of GaAs as a Function of Wavelength	7
2	Doping Dependence of Electron Diffusion Length and Lifetime in p-type GaAs	9
3	Doping Dependence of Hole Diffusion Length and Lifetime in n-type GaAs	10
4	Calculated Values of Efficiency, Short-Circuit Current and Open-Circuit Voltage of P/N Cell versus Surface Layer Doping for x_j = 0.2 μm	11
5	Calculated Values of Efficiency, Short-Circuit Current and Open-Circuit Voltage of P/N Cell versus Surface Layer Doping for x_j = 0.4 μm	12
6	Calculated Values of Efficiency, Short-Circuit Current and Open-Circuit Voltage of P/N Cell versus Surface Layer Doping for x_j = 0.6 μm	13
7	Calculated Values of Efficiency, Short-Circuit Current and Open-Circuit Voltage of P/N Cell versus Surface Layer Doping for x_j = 0.8 μm	14
8	Calculated Values of Efficiency, Short-Circuit Current and Open-Circuit Voltage of P/N Cell versus Surface Layer Doping for x_j = 1.0 μm	15
9	Variation of Calculated Efficiency, Short-Circuit Current and Open-Circuit Voltage with Junction Depth for a Range of Surface Layer Concentrations	17
10	Variation of Calculated Efficiency, Short-Circuit Current and Open-Circuit Voltage with Junction Depth for a Range of Base Region Concentrations	18
11	Calculated Values of Efficiency, Short-Circuit Current and Open-Circuit Voltage of N/P Cell versus Surface Layer Doping for Several Values of Junction Depth	20
12	Calculated Values of Efficiency, Short-Circuit Current and Open-Circuit Voltage of N/P Cell versus Surface Layer Doping for Several Values of Junction Depth	21

LIST OF ILLUSTRATIONS (Concluded)

Figure		Page
13	Calculated Values of Efficiency, Short-Circuit Current and Open-Circuit Voltage versus Junction Depth for Several Values of Base Doping.	22
14	Range-Energy Relation for Zinc in GaAs	26
15	Dopant Concentration Distribution of Zinc in GaAs for Several Implantation Energies	27

SECTION 1
INTRODUCTION

In the past GaAs solar cells have received considerable attention as an attractive alternative to Si cells for achieving higher efficiencies, higher temperature operation and increased resistance to radiation in the outer space environment. These predicted improvements were based on the bulk material characteristics of GaAs. Nearly all of the solar cell development effort occurred during the early stages of material and device process development with the result that the performance of the best cells reached 13% efficiency.[1, 2] About the time work on GaAs solar cell development was de-emphasized, increased attention to other GaAs devices began to develop, the collective results of which have contributed to significant improvements in both materials technology and p-n junction formation processes.[3]

Recent experimental and theoretical work on GaAs photodiodes and solar cells, respectively, indicate that high efficiency solar cells (greater than 20%) in GaAs are possible with present material and process technology. Detailed review of this work and additional calculations and considerations taking into account practical process limitations confirm this conclusion and form the basis for the present program.

The program has been divided into three phases with each phase designed to provide results which are complete, and will provide the necessary input to conduct the succeeding phase. The three phases are as follows:

(a) Phase I - Analytical

- Refinement of calculations of GaAs solar cell output parameters.
- Development of computer model for parameter optimization.

(b) Phase I - Experimental

- Determination of optimum implantation parameters.
- Determination of optimum contact metallurgy, antireflective coating and surface treatment.

(c) Phase II - Fabrication

- Fabrication and characterization of first lot of development solar cells.

(d) Phase III - Fabrication

- Refinement of implantation parameters for maximum solar cell efficiency.
- Refinement of processing steps for maximum efficiency.
- Fabrication and characterization of a second lot of developmental solar cells.
- Radiation hardness study.

Phase I (analytical) will produce the values required to specify the material characteristics desired for both cell type polarities. These specifications will be used as a guide in conducting the experimental part of Phase I. The results of Phase I (experimental) will produce data on the optimum process parameters to be incorporated into fabricating the first lot of developmental solar cells. Upon characterization of these cells refinements will be made to the initial process procedures based on the results obtained. A second lot of developmental cells will then be fabricated and characterized as part of Phase III. A radiation hardness study of these cells will conclude the work in Phase III.

This report covers the results of Phase I - analytical. The formulations to determine solar cell output have been incorporated into a computer model for cell optimization study. The results have been analyzed with the following principal conclusions:

- Cell output is higher for the P/N polarity than for the N/P polarity.

- Both cell polarities show efficiency to have a larger dependence on short-circuit current than on open-circuit voltage under nearly all conditions considered.
- The tolerances and requirements of a cell fabrication process are more critical for an N/P type than for a P/N type cell.
- A cell efficiency of 20% should be possible in GaAs.

These conclusions and others are discussed in more detail in this report. A brief discussion of the various considerations concerning the fabrication of ion implanted junctions is also given. Here several factors such as range-energy, dopant profiles, annealing, etc., affecting the doping of GaAs by this technique are discussed. Results of experimental investigation of the optimum implantation and other solar cell process parameters will be discussed in the next report.

SECTION 2
COMPUTER MODEL

The computer model developed for optimization of the important parameters affecting GaAs solar cell output performance consists essentially of the formulations of Moss.[2, 4] The relations derived in the references which describe solar cell behavior are as follows:

$$J_T = J_{SC} - j_o \left(e^{qV/nkT} - 1\right) - J_{rec}$$

$$J_{SC} = \int_{\lambda_1}^{\lambda_2} J_o \, d\lambda$$

$$J_o = \frac{IKL}{(K^2 L^2 - 1)}$$

$$\left[\frac{2(\alpha + KL) - e^{-Kt}\left\{e^{t/L} - e^{-t/L}\right) + \alpha \left(e^{t/L} + e^{-t/L}\right)\right\}}{\left(e^{t/L} + e^{-t/L}\right) + \alpha \left(e^{t/L} - e^{-t/L}\right)} -$$

$$\frac{e^{-Kt}\left(KL + \ell/L\right)}{(1 + K\ell)} \right]$$

$$J_{rec} = \frac{2 n_i kT}{\tau} \quad \frac{W}{(V_D - V_L)} \quad \sinh \left(\frac{e V_L}{2kT}\right) \quad \text{cosecx} \tan^{-1}$$

$$\left\{ \tan \frac{x}{2} \quad \tanh \frac{e}{2kT} \quad (V_D - V_L) \right\}$$

$$j_o = q n_i^2 \left[\frac{1}{N_A} \frac{t}{\tau_n} + \frac{1}{N_D} \frac{L_p}{\tau_p} \right]$$

$$V_{oc} = \frac{kT}{q} \ln J_o/j_o$$

$$V_L = r\left(\frac{kT}{q}\right)$$

$$J_L = J_o \left(\frac{r}{r+1}\right)$$

$$J_o/j_o = (r+1)\, e^r$$

$$\eta = \frac{V_L J_L}{P_{in}}$$

where: J_T = total current

J_o = short circuit current density

j_o = reverse saturation current density

I = incident photon flux

t = junction depth

K = absorption coefficient

L = minority carrier diffusion length

V_{oc} = open circuit current voltage

τ = minority carrier lifetime

V_L = operating voltage

V_D = built in junction voltage

J_L = operating current density

s = surface recombination velocity

N_A, N_D = majority carrier concentrations

W = depletion layer width

From these equations it is clear that J_o and j_o are the important quantities to consider in optimizing cell performance. The material characteristics which affect these two quantities are minority carrier diffusion length and lifetime, majority carrier concentration, and surface recombination velocity. Cell fabrication considerations affecting output include junction depth, junction recombination current and surface recombination velocity. In the present model we assume junction recombination to be small and have assigned as value of 10^5 cm sec^{-1} to the surface recombination velocity while varying junction depth. Thus the material characteristics can be optimized and a cell structure determined for experimental study of the cell fabrication process. The validity of these assumptions will be determined by the results of the experimental work and the ability of the process to produce the required values. Losses due to reflection and series resistance have been neglected as well as the effects of a built-in drift field which should compensate somewhat for these losses. Expected reduction in the computed values for the various cell parameters should not exceed 10% due to these factors. The above relations are for a P on N cell polarity which were modified in the appropriate manner to consider also the N on P cell polarity.

The computer program inputs required for the various constants and material parameters were taken from the literature. Figure 1 contains the absorption coefficient of GaAs versus wavelength[5, 6] used together with the solar-irradiance data of Johnson[7] in performing the integration to obtain (J_{SC}). Integrating the total number of photons available for electron-hole pair

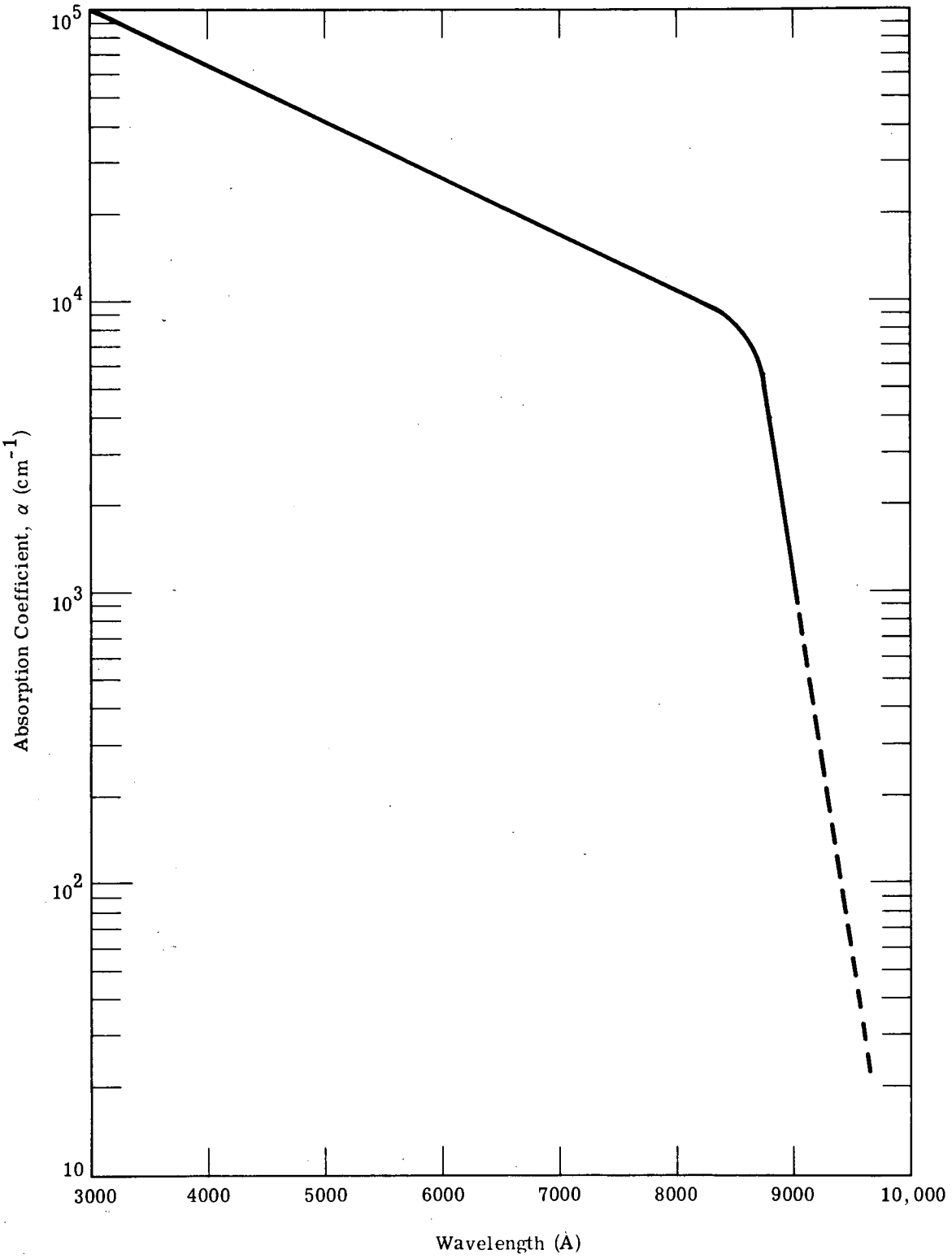

Figure 1. Absorption Coefficient of GaAs as a Function of Wavelength.

1-6334

production between 3000 and 9000 Å yields a value of 2.5×10^{17} photons cm^{-2}. Considering the relation between absorption coefficient and the distance from the surface where radiation is absorbed $\left(d = \frac{1}{\alpha} \text{ cm}\right)$, this curve shows that photons which contribute to power generation in GaAs are absorbed within 5 μm of the surface. Figures 2 and 3 contain curves for minority carrier lifetime and diffusion length for electrons and holes respectively as functions of majority carrier concentration. The curves in Figure 3 were taken from reference (8). Similar curves for electrons were derived from bulk mobility data of Sze and Irvin[9] assuming the values apply to minority carriers moving in a region of opposite type with the same concentration of electrically active impurities. In addition, the lifetime was assumed constant for $10^{16} < N_A < 10^{19}$ and varied for $N_A > 10^{19}$ according to a constant lifetime - carrier concentration product, $\tau_n N_A = 10^{10}$ suggested by Moss.[4]

Both lifetime and diffusion length were assumed constant throughout the region of interest in the cell.

2.1 Computer Model Results

Computer calculations were made for both cell polarities to determine a cell design which would specify the material characteristics required for maximum efficiency. The parameters varied included carrier concentration, both in the surface and base regions, and therefore minority carrier lifetime and diffusion length, and junction depth. A surface recombination velocity value of 10^5 cm sec^{-1} was assigned for both cases, a value achieveable with a practical cell process. Generally, the calculations were limited to a range of values for the parameters varied which reflect the influence of practical constraints on material properties and/or process considerations.

2.1.1 P/N Cell Polarity

Figures 4 through 8 show computed values of efficiency (η), short-circuit current (J_{SC}) and open-circuit voltage (V_{oc}) for P/N cells as functions of surface layer and base region carrier concentration for several values of

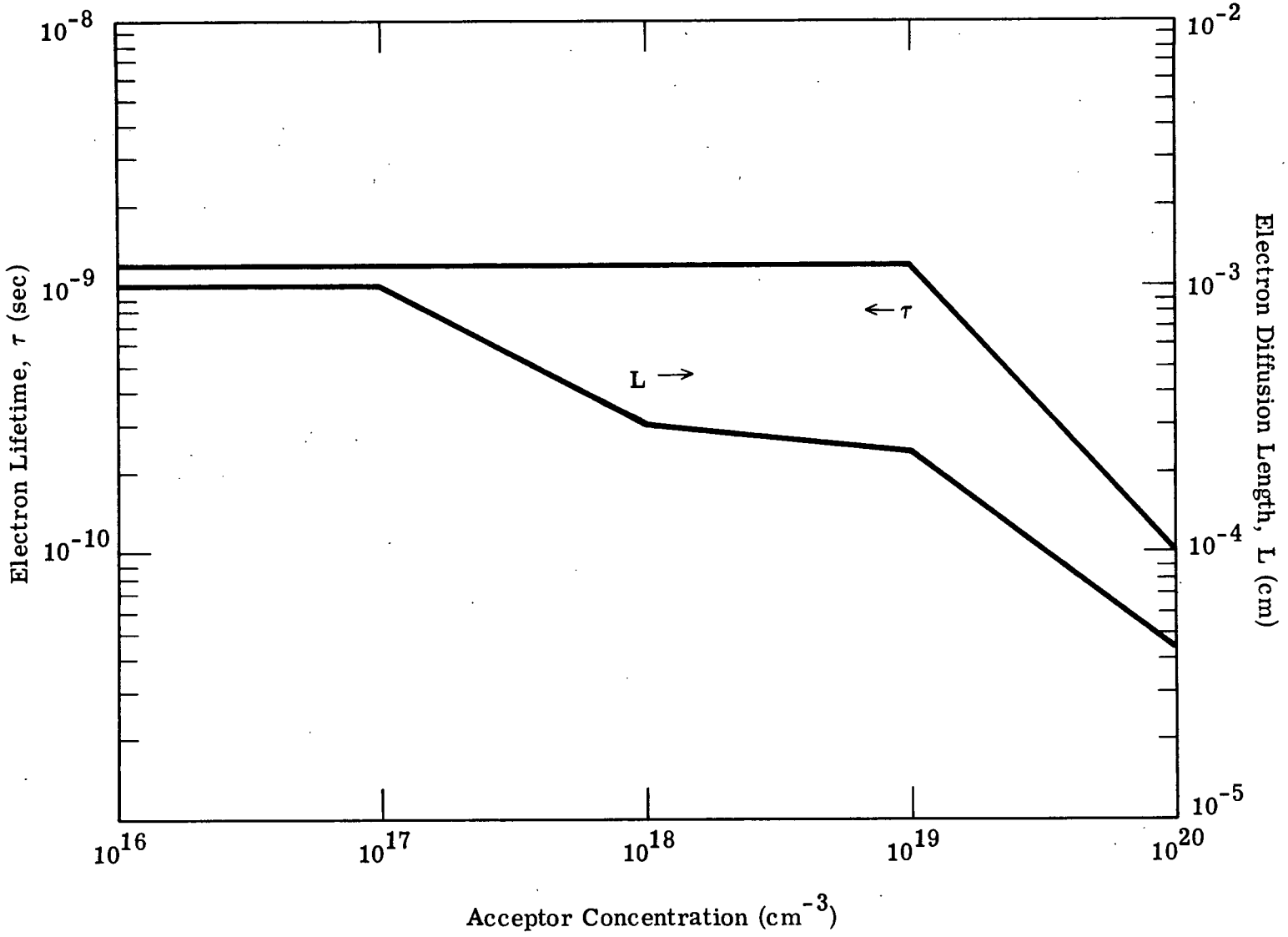

Figure 2. Doping Dependence of Electron Diffusion Length and Lifetime in p-type GaAs.

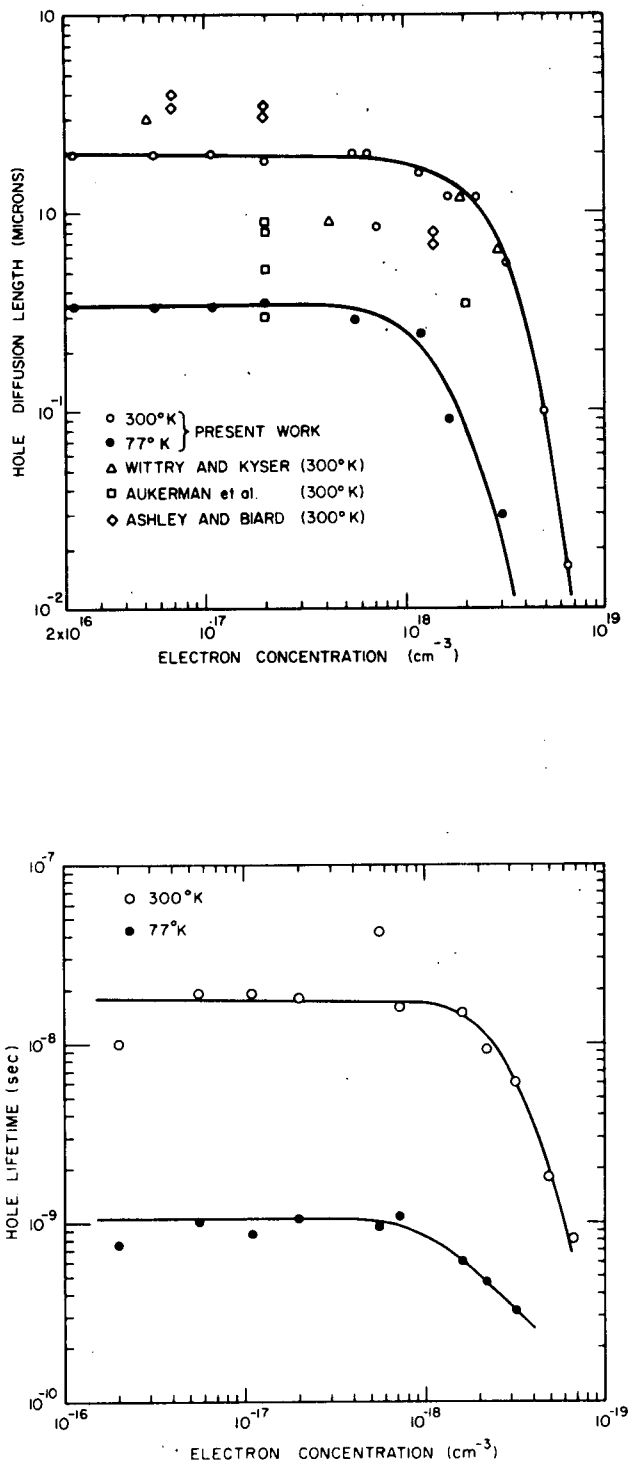

Figure 3. Doping Dependence of Hole Diffusion Length and Lifetime in n-type GaAs.

1-6336

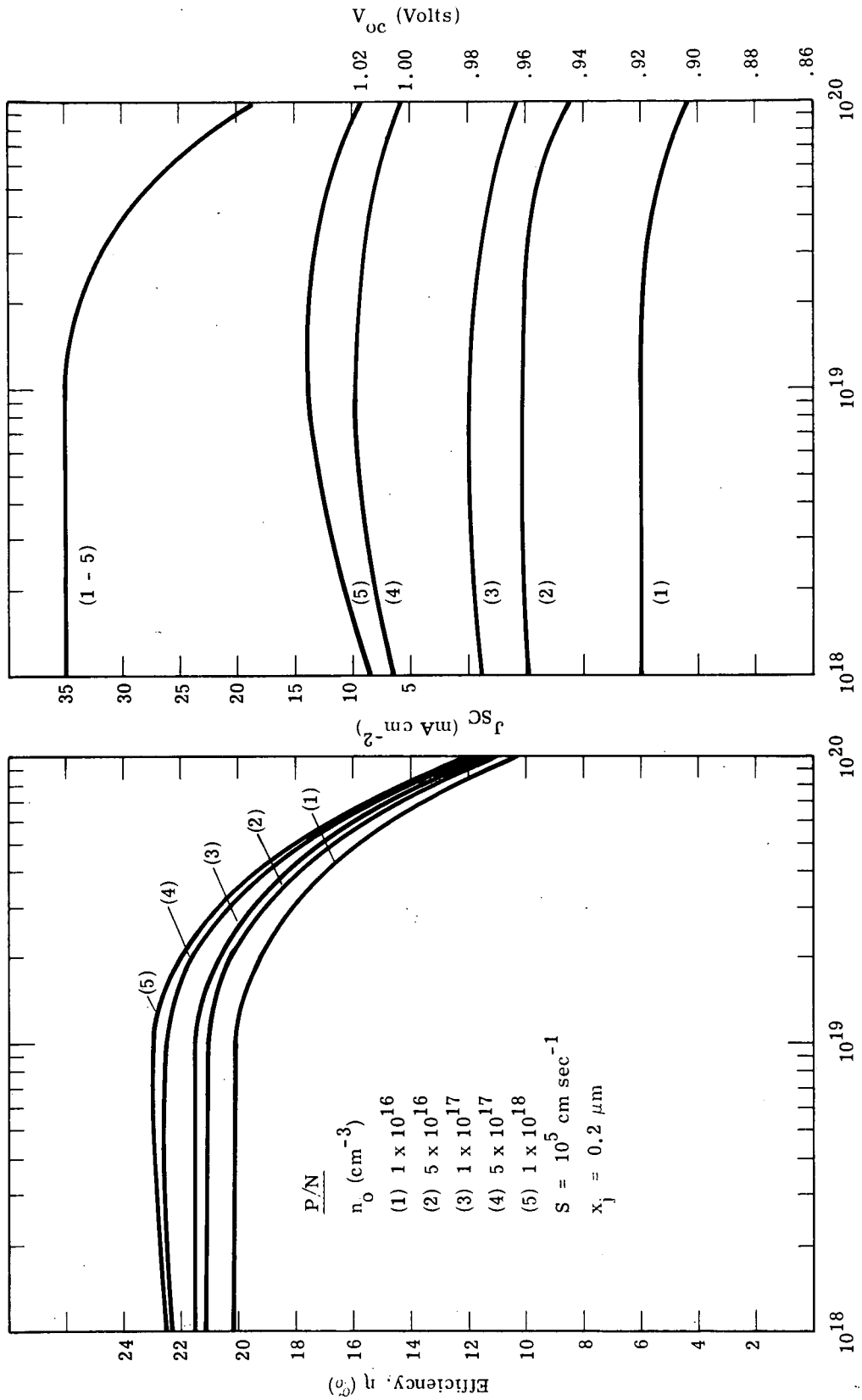

Figure 4. Calculated Values of Efficiency, Short-Circuit Current and Open-Circuit Voltage of P/N Cell versus Surface Layer Doping for x_j = 0.2 μm.

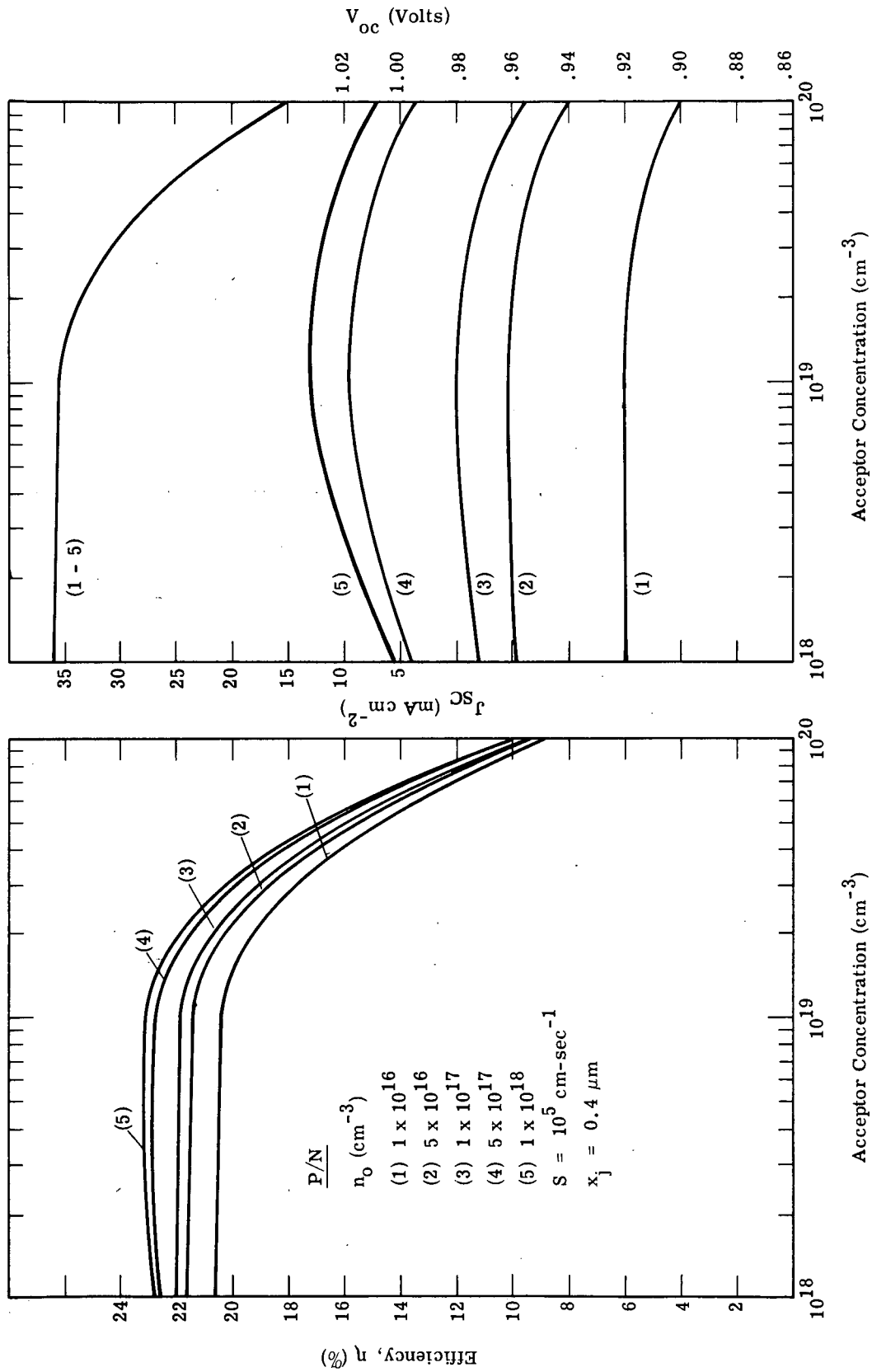

Figure 5. Calculated Values of Efficiency, Short-Circuit Current and Open-Circuit Voltage of P/N Cell versus Surface Layer Doping for x_j = 0.4 μm.

1-6338

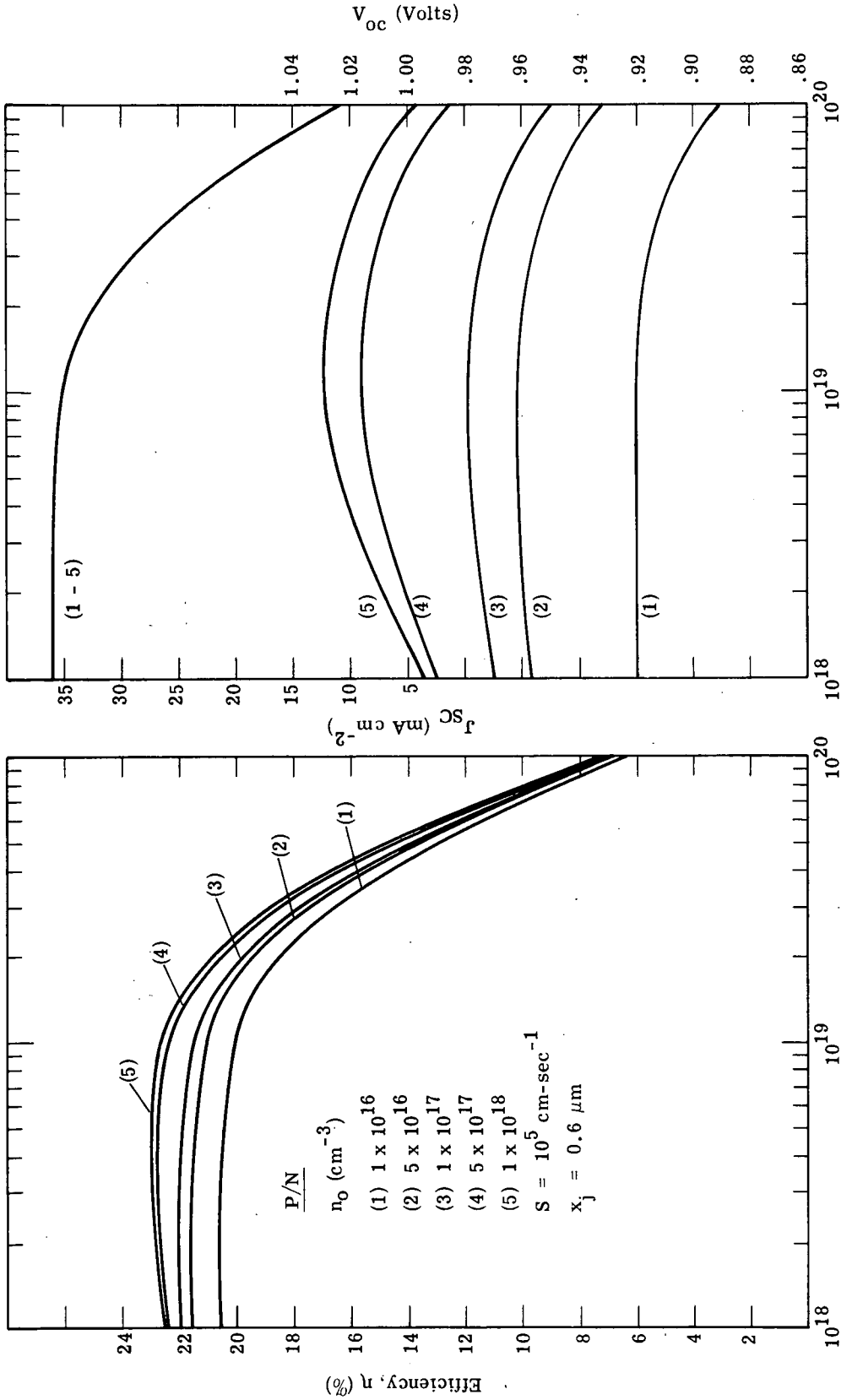

Figure 6. Calculated Values of Efficiency, Short-Circuit Current and Open-Circuit Voltage of P/N Cell versus Surface Layer Doping for x_j = 0.6 μm.

1-6339

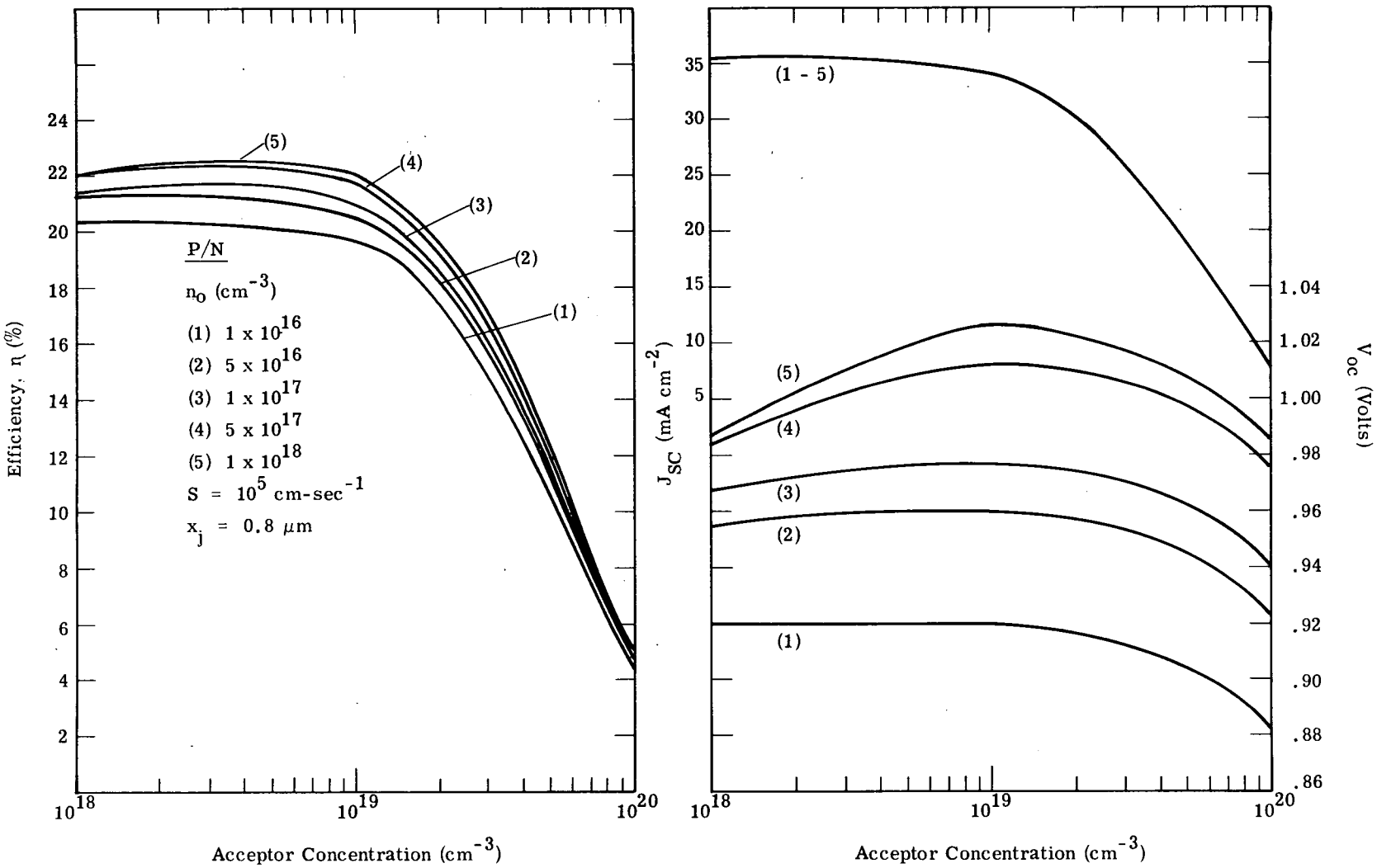

Figure 7. Calculated Values of Efficiency, Short-Circuit Current and Open-Circuit Voltage of P/N Cell versus Surface Layer Doping for x_j = 0.8 μm.

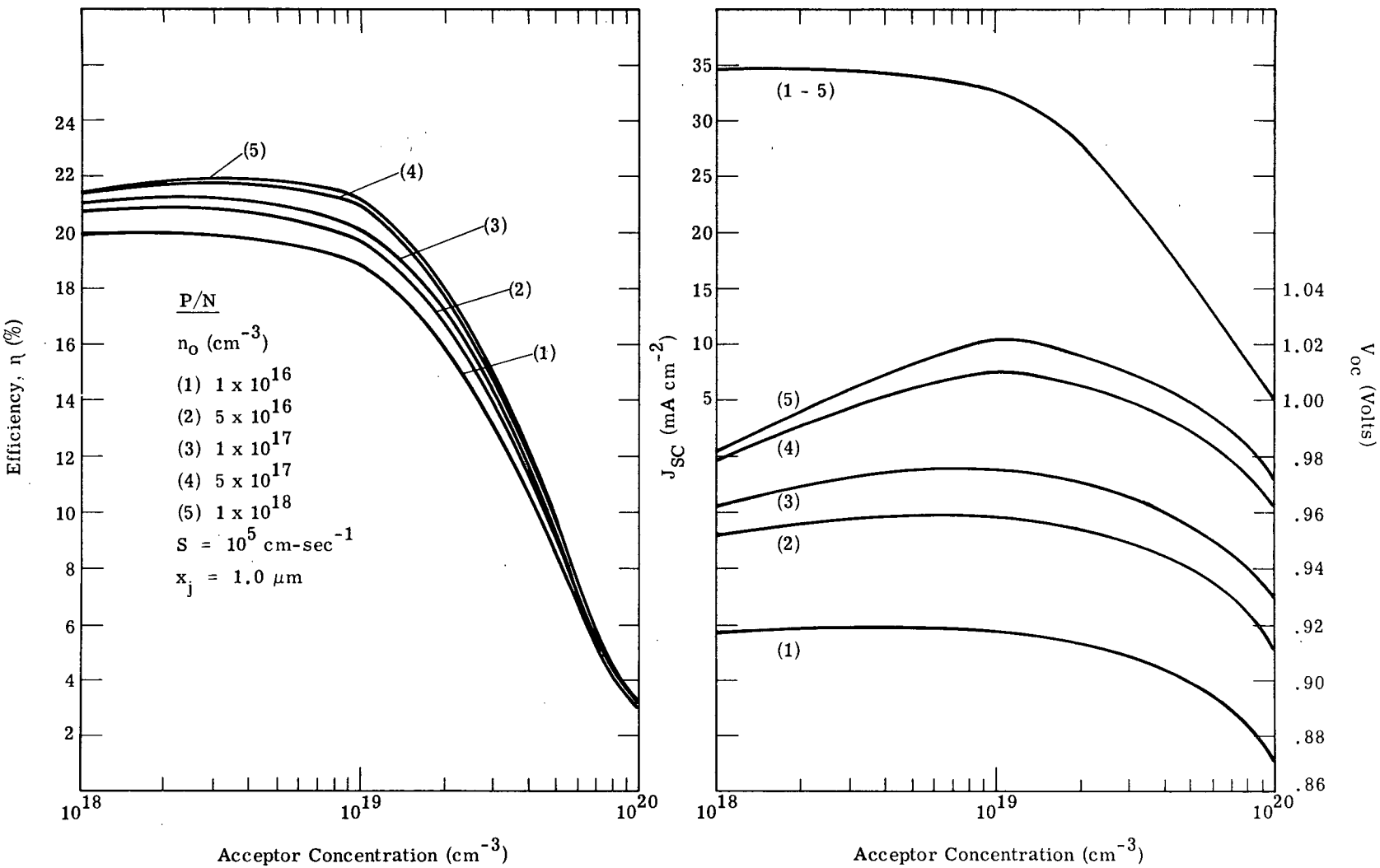

Figure 8. Calculated Values of Efficiency, Short-Circuit Current and Open-Circuit Voltage of P/N Cell versus Surface Layer Doping for x_j = 1.0 μm.

junction depth. The family of curves in each figure represent the cell output for a range of n-type base region carrier concentrations (10^{16} - 10^{18} cm^{-3}) plotted against surface concentrations ranging between 10^{18} cm^{-3} and 10^{20} cm^{-3}. The curves show that efficiency increases with base doping due to higher open circuit voltage and lower saturation current density (j_o). The short circuit current density is independent of base doping indicating a sufficiently large hole diffusion length for high collection efficiency in the base region. A maximum cell output occurs with surface layer doping of approximately 10^{19} cm^{-3}, above this value output rapidly falls off. As the figures show, this fall off in efficiency is due chiefly to a reduced short circuit current density which in turn is a consequence of smaller electron diffusion lengths. This trend is independent of junction depth but is more pronounced as the junction depth increases.

To show more clearly the influence of junction depth on output characteristics, Figures 9 and 10 contain curves showing cell output as a function of junction depth for a range of surface and base region carrier concentrations, respectively. In Figure 9, the surface concentration was varied between 10^{18} cm^{-3} and 10^{20} cm^{-3} for a base doping of 10^{18} cm^{-3} and junction depths between 0.2 and 1.0 microns. Efficiency shows a small drop for surface concentrations up to 2×10^{19} cm^{-3} for these junction depths; above 2×10^{19} cm^{-3} the decrease in efficiency is accelerated becoming increasingly dependent on junction depth. Examination of the open-circuit voltage (V_{oc}) and short-circuit current density (J_{SC}) curves in the figure show the decrease in efficiency is due to a reduction in (V_{oc}) for the lighter surface doping which gradually shifts to a dependence on (J_{SC}) as the surface layer doping increases. In Figure 10 for a surface layer concentration of 10^{19} cm^{-3} (which appears to be near optimum) the cell output shows little dependence on junction depth for all base region carrier concentrations considered. Again the fall off in efficiency for junction depths approaching one micron is due to the decrease in (J_{SC}). These curves show the optimum junction depth to be $\sim$0.4 micron; and for a base doping of 10^{18} cm^{-3} a cell efficiency of 23.1% is calculated. It is significant to note that nearly all the efficiency curves lie above 20% with only the

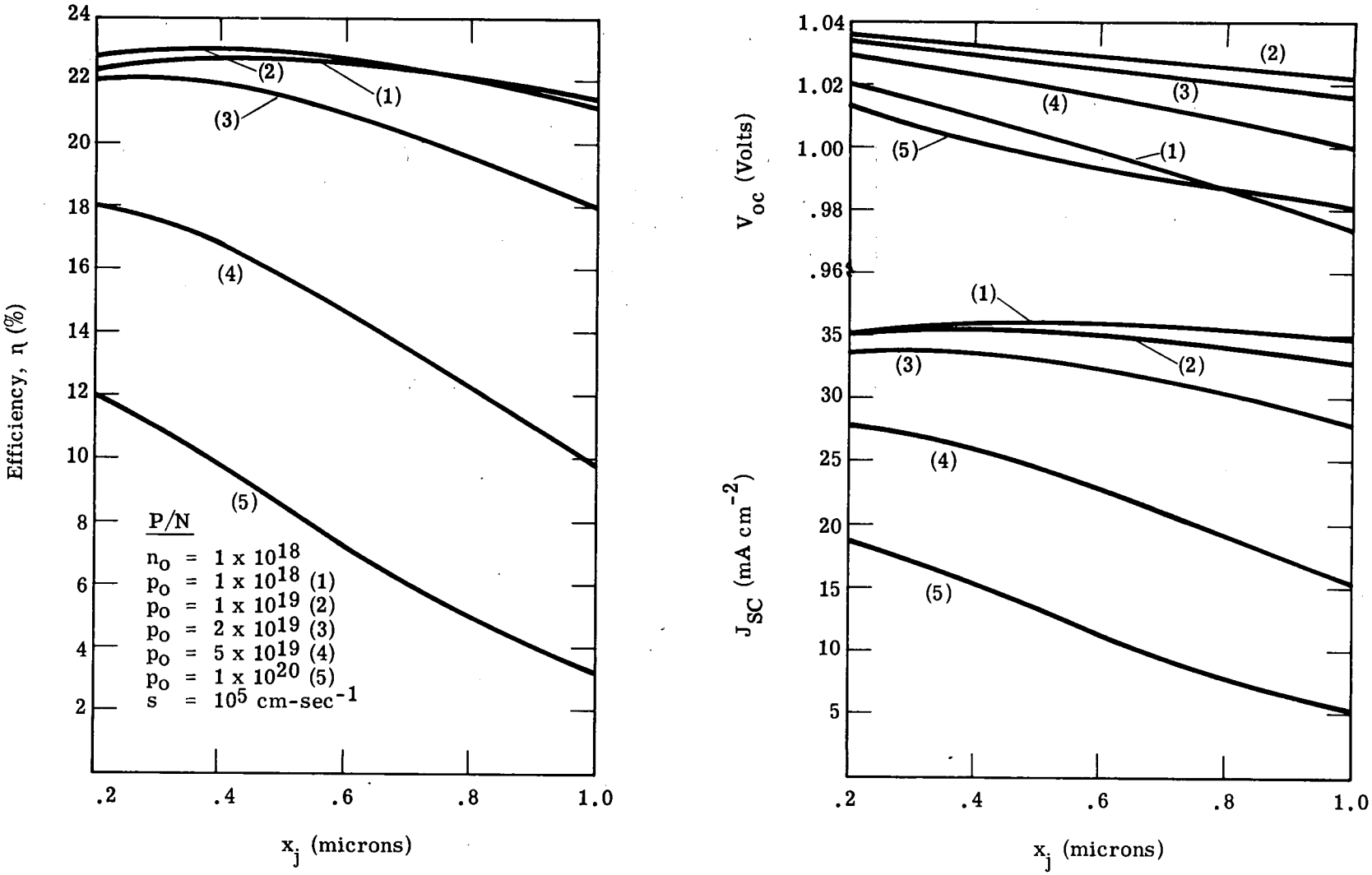

Figure 9. Variation of Calculated Efficiency, Short-Circuit Current and Open-Circuit Voltage with Junction Depth for a Range of Surface Layer Concentrations.

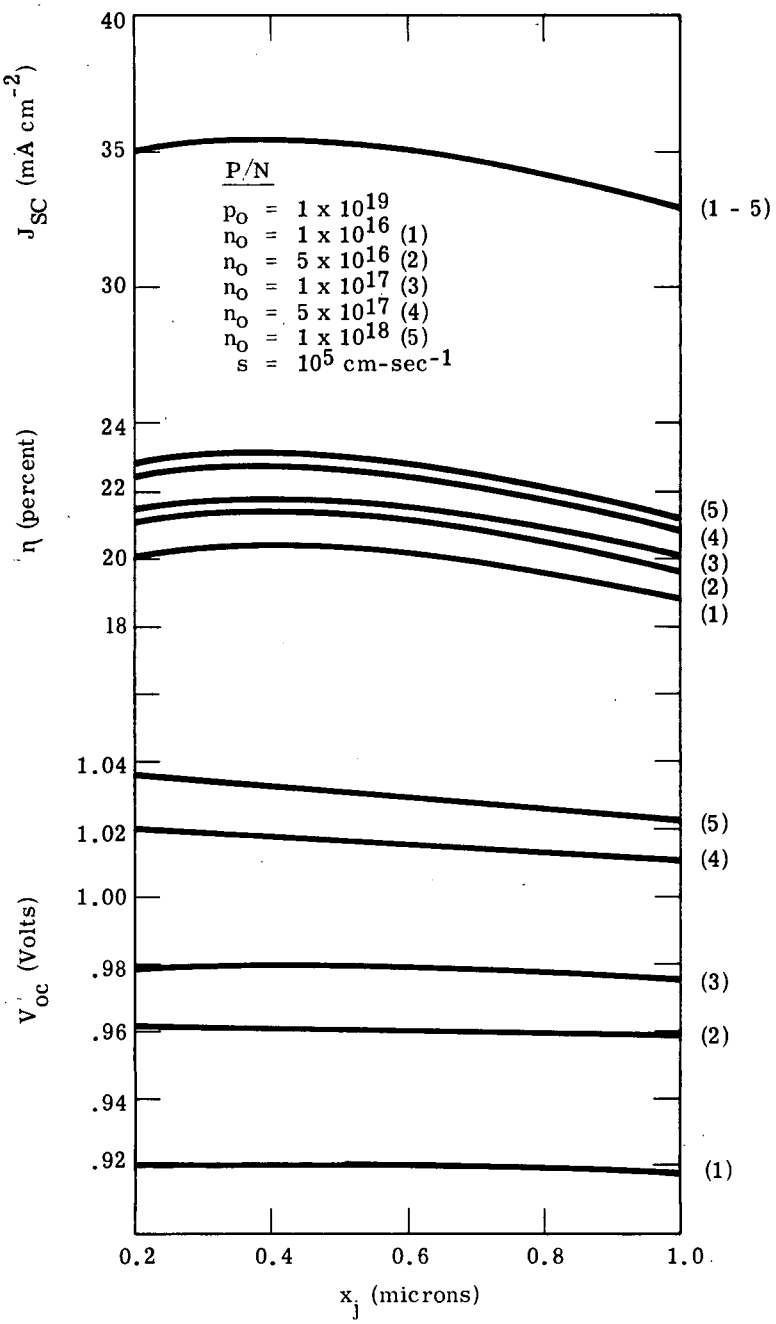

Figure 10. Variation of Calculated Efficiency, Short-Circuit Current and Open-Circuit Voltage with Junction Depth for a Range of Base Region Concentrations.

1-6343

smallest base concentration droping below this value as the junction depth increases. This indicates that the principal consideration in fabricating a cell incorporating these characteristics should be the transverse resistance of the surface region for optimizing output.

2.1.2 N/P Cell Polarity

Figures 11 through 13 present similar calculated results for the N/P cell polarity. The range in surface layer doping is not as large as the P/N cell polarity due to the upper limit in n-type doping of approximately 5×10^{18}, a characteristic of GaAs material. As the curves in Figure 3 indicate, hole lifetime and diffusion length are significantly reduced in this concentration region making consideration of a cell with surface layer concentrations greater than $\sim 2 \times 10^{18}$ impractical. In Figure 11, curves for the three cell outputs (η, V_{oc}, J_{SC}) are plotted against surface layer doping for a base doping of 10^{16} cm-^{3} and several values of junction depth. All curves exhibit reduced values above surface layer concentrations of 10^{18} cm^{-3}, a consequence of reduced hole lifetime and diffusion length. This is consistent with the increase in efficiency as the junction moves closer to the surface. The efficiency curves are influenced for the most part by the behavior of (J_{SC}). Figure 12 contains similar curves for base region doping of 10^{17} cm^{-3}. The trends shown by these curves are the same as the previous figure with a small improvement in (η) and (V_{oc}) due to a lower saturation current density (j_o). Figure 13 shows the three cell parameters as a function of junction depth for surface layer carrier concentration of 10^{18} cm^{-3} and several base concentrations. The short circuit current density is quite sensitive to junction depth whereas open-circuit voltage is more sensitive to base region doping. In fabricating an optimized cell of this type a careful trade-off in junction depth versus transverse resistance would be required.

2.1.3 Conclusions

From the results of the above calculations the following observations are made:

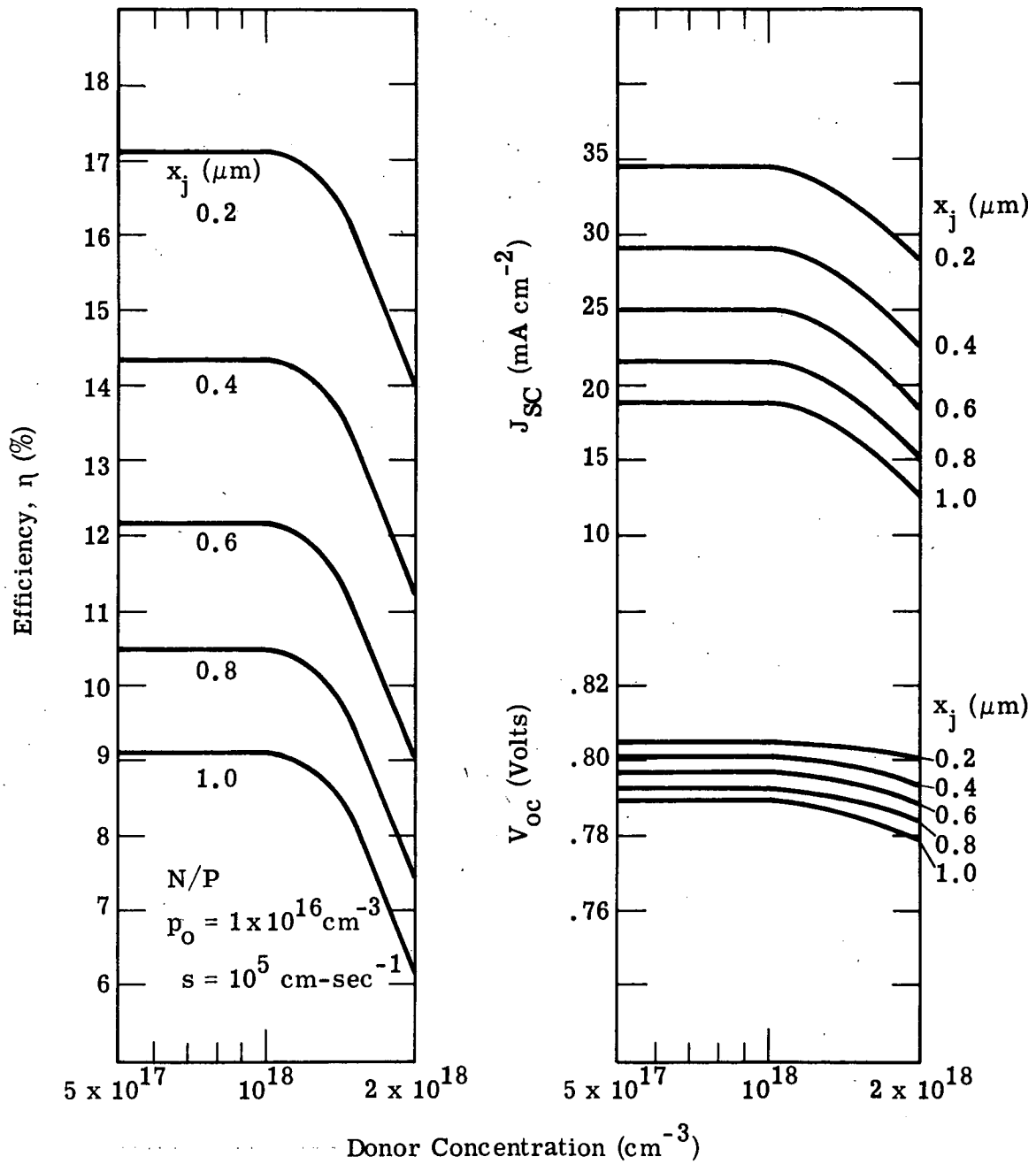

Figure 11. Calculated Values of Efficiency, Short-Circuit Current and Open-Circuit Voltage of N/P Cell versus Surface Layer Doping for Several Values of Junction Depth.

1-6344

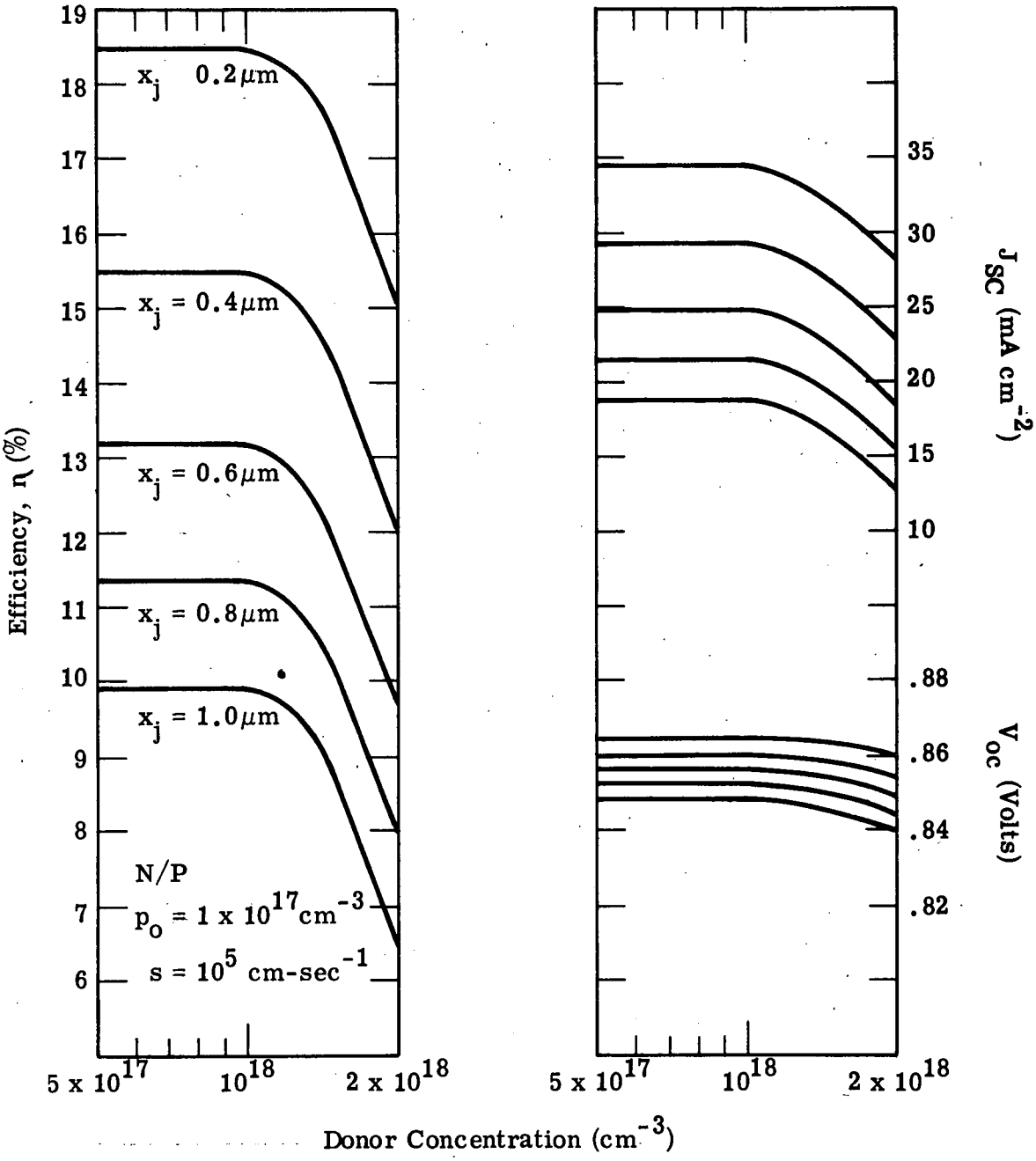

Figure 12. Calculated Values of Efficiency, Short-Circuit Current and Open-Circuit Voltage of N/P Cell versus Surface Layer Doping for Several Values of Junction Depth.

1-6345

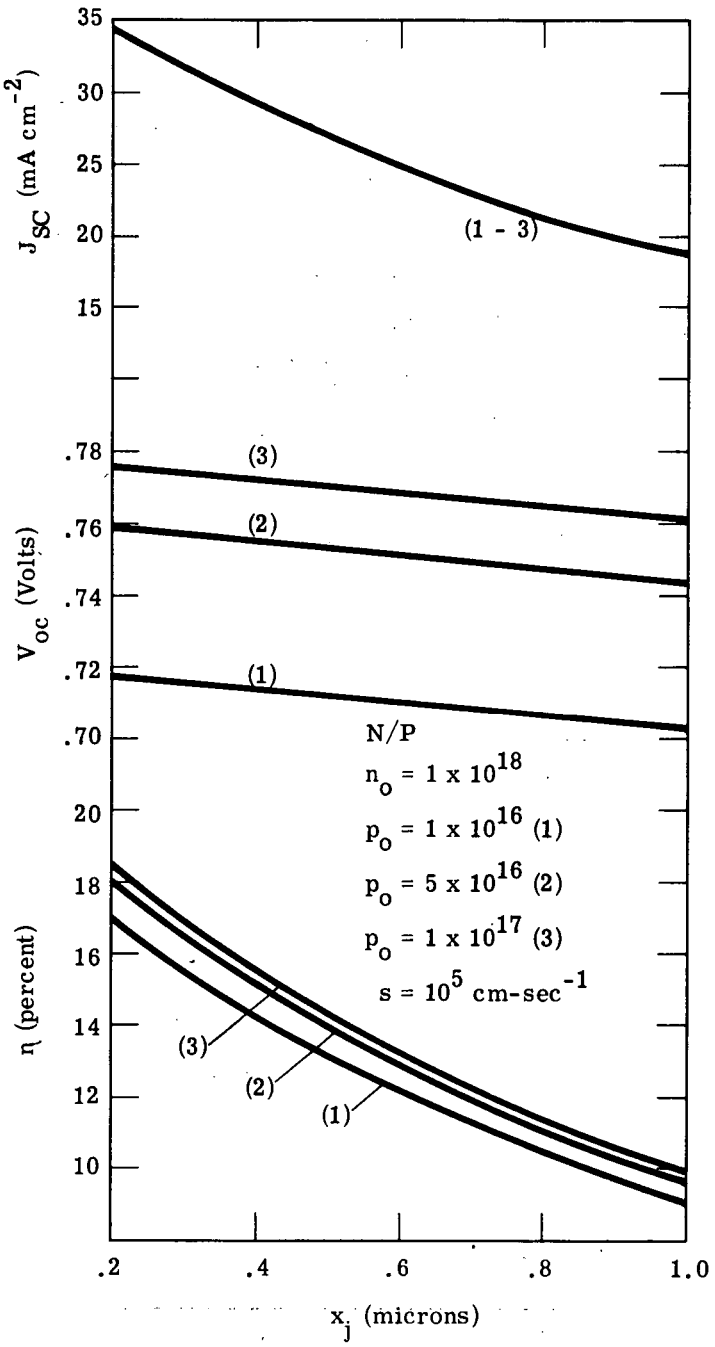

Figure 13. Calculated Values of Efficiency, Short-Circuit Current and Open-Circuit Voltage versus Junction Depth for Several Values of Base Doping.

1-6346

- For P/N cell polarity a near optimum structure consists of surface layer doping of 10^{19} cm^{-3}, base region doping of 10^{18} cm^{-3}, and junction depth 0.4 microns.
- Considerable latitude exists for adjusting dopant concentrations and junction depth in fabrication of a P/N cell.
- For N/P cell polarity a near optimum structure consists of surface layer doping of 10^{18} cm^{-3}, base region doping of 10^{17} cm^{-3}, and junction depth of 0.2 μm.
- Short-circuit current density for N/P cell is more sensitive to junction depth than P/N cell.
- Open-circuit voltage is primarily sensitive to base concentration for both cell polarities.
- Both cell polarities show efficiency to be more dependent on short-circuit current than on open-circuit voltage under nearly all conditions.
- Encorporation of a drift field in the surface layer in both cell polarities will improve cell output which can compensate for losses due to resistance, reflection and junction effects not explicitly considered in these calculations.
- Particular attention should be given to the factors affecting minority carrier lifetime and diffusion length in the experimental work and cell fabrication.
- The tolerances and requirements of a cell fabrication process are more critical for the N/P cell than for the P/N cell.

SECTION 3
SOLAR CELL FABRICATION CONSIDERATIONS

The ion implantation technique for junction formation will be studied under this program for solar cell fabrication. Zinc and selenium dopants have been chosen to form the p- and n-type surface regions, respectively, using commercially available GaAs material. The experimental areas of investigation for determining the optimum parameters for the cell fabrication process include the following:

(1) Surface and base region thickness, doping level and doping profile which provide optimum efficiency;
(2) Influence of fabrication parameters on junction quality (abruptness, reverse saturation current, A-factor) as required for optimum efficiency;
(3) Material and contact requirements necessary to minimize series resistance;
(4) Nature of material and process-induced defects (bulk, junction and surface) responsible for limiting efficiency, and practical means for minimizing recombination and optimizing cell efficiency;
(5) Other physical parameters (e.g., minority carrier diffusion lengths) necessary to analyze experimental cell performance in terms of the analytical model

3.1 P/N Junction Formation

The major process considerations in constructing an ion implanted GaAs solar cell are the range-energy relation for achieving the desired junction depth, carrier concentration and distribution, and process induced defects affecting surface layer and junction perfection. Junction depth can be determined from range-energy calculations using the LSS theory. Calculated values for zinc in

GaAs are shown in Figure 14. The curve labeled R_p is the projected range or the peak of the implanted dopant distribution which is gaussian according to theory. The curve labeled x_j, represents the junction depth for a ratio of peak surface layer doping to base region doping of 100. The latter curve will vary according to the formulas for gaussian distributions and will produce deeper junctions for larger dopant ratios.[10] Figure 15 shows the predicted distributions for three implantation energies. The peak concentration of 2×10^{19} cm^{-3} and the implant energies were selected for illustration and represent the approximate region of interest in our experimental work. By inserting a base doping concentration on the curves junction depths can be determined at the intersection with the implanted distribution. Similar curves for selenium can also be constructed; which because of its similarity to zinc in atomic number and mass will not differ greatly from the curves for zinc.

The peak impurity concentration is related to the implanted dose by the relation

$$\hat{N} = \frac{0.4\, N_{\square}}{\Delta R_p}$$

where: $\hat{N}$ = peak concentration

$N_{\square}$ = ion dose

ΔR_p = standard deviation in projected range

In the present work since ΔR_p ranges between .05 - .1 μm and N approximately 2×10^{19} cm^{-3}, zinc doses of approximately 10^{15} cm^{-2} will be required. A selenium dose of approximately 5×10^{14} cm^{-2} would be required to produce an n-type layer of $\sim 2 \times 10^{18}$ cm^{-3}.

Additional considerations for experimental investigation include post-implantation annealing to remove radiation damage effects and produce the desired p^+ or n^+ surface layer. Previous experience indicates

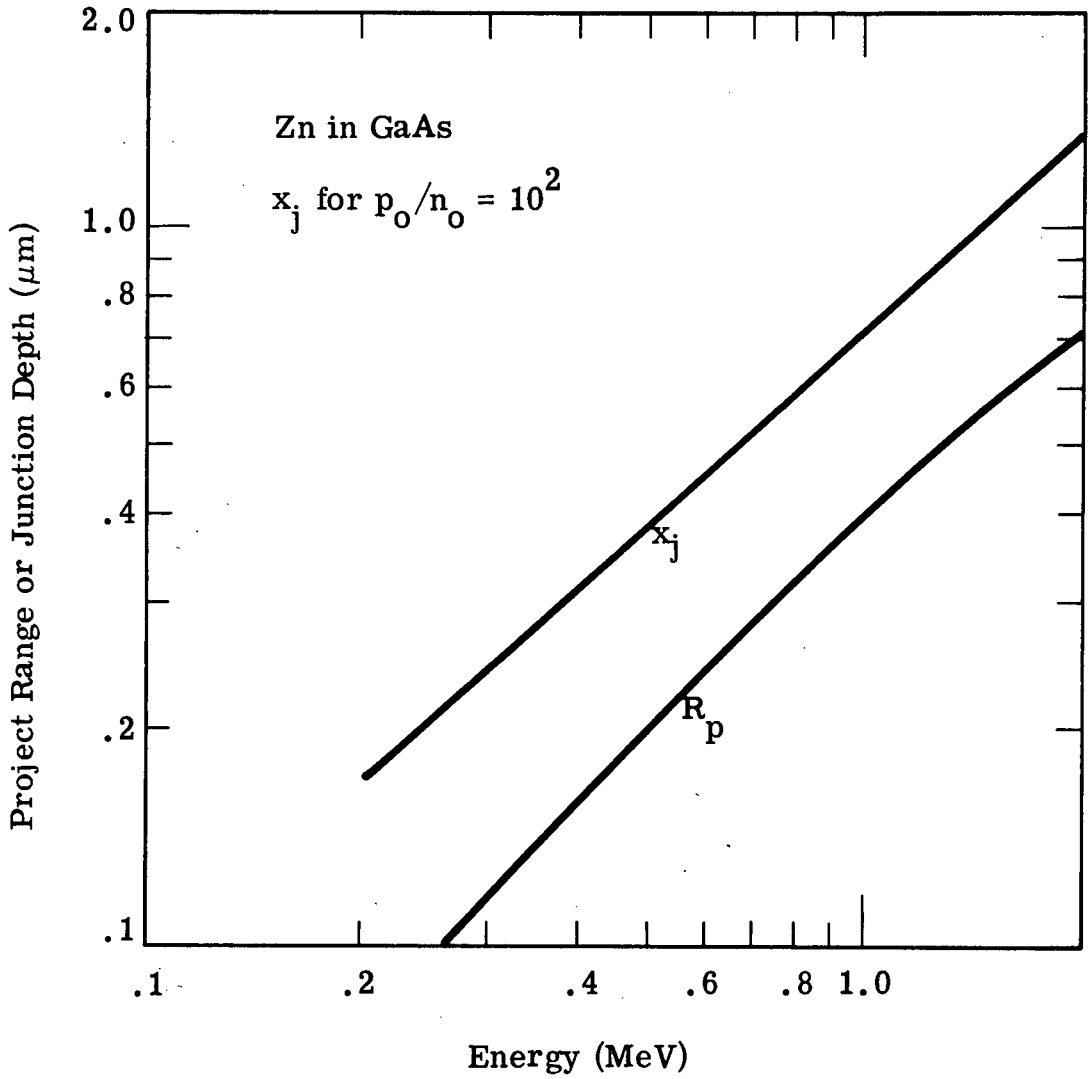

Figure 14. Range-Energy Relation for Zinc in GaAs.

1-6347

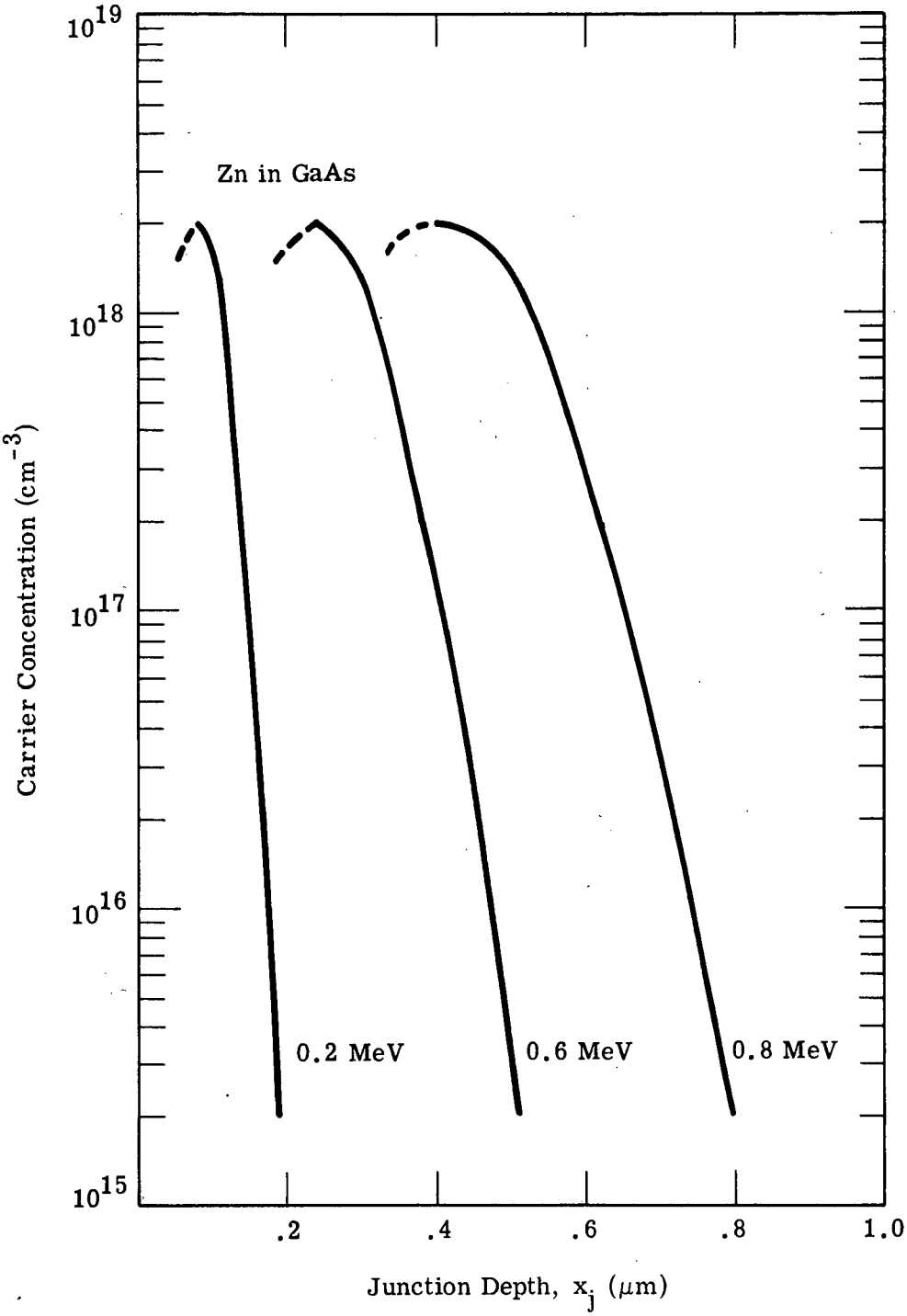

Figure 15. Dopant Concentration Distribution of Zinc in GaAs for Several Implantation Energies.

1-6348

that anneal temperatures between 600 ° - 900 ℃ should be the region of concentration. The theoretical predictions assume gaussian distributions and 100% dopant utilization which must also be verified.

SECTION 4
FUTURE WORK

The next report period will be concerned with experimental investigation of the optimum implantation and cell process parameters required to achieve the cell structure suggested by the analytical results. This will involve investigation of range-energy, surface preparation and contact metallurgy and characterization of implanted surface layer and junction behavior.

REFERENCES

1. Gobat, A. R., et. al., IRE Trans. on Mil. Electron, 6, 20 (1962).

2. Ellis, B. and Moss, T. S., Solid State Electron, 13, 1, (1970).

3. See for example, Gallium Arsenide - Proc. Symp. Institute of Phys. and Phys. Society, London (1966, 1968, 1970); Semiconductors and Semimetals ed. by R. K. Willardson and A. C. Beer, Vol. 7, Parts A and B, Academic Press, New York (1971).

4. Moss, T. S., Semiconductors and Semimetals, ed. by R. K. Willardson and A. C. Beer, Vol. 2, Academic Press, New York (1966).

5. Kudman, I. and Seidel, T., J. of Appl. Phys., Vol. 33, No. 3, 771-773, (March 1962).

6. Hwang, C. J., J. of Appl. Phys., Vol. 40, No. 11, 4591-4597, (October 1969).

7. Johnson, F. S., J. Meteor. 2, 431 (1954).

8. Hwang, C. J., J. of Appl. Phys. Vol. 42, No. 11, 4412-4413, (October, 1971).

9. Sze, S. M. and Irvin, J. C., Solid State Electron, Vol. II, 599-602 (1968).

10. See for example, Gibbons, J. F., Proc. IEEE, Vol. 56, No. 3, 305 (March 1968).